Adherent carbon film deposition by cathodic arc with implantation

E. G. Gerstner, D. R. McKenzie, M. K. Puchert, P. Y. Timbrell, and J. Zou

Citation: Journal of Vacuum Science & Technology A **13**, 406 (1995); doi: 10.1116/1.579372

View online: http://dx.doi.org/10.1116/1.579372

View Table of Contents: http://scitation.aip.org/content/avs/journal/jvsta/13/2?ver=pdfcov

Published by the AVS: Science & Technology of Materials, Interfaces, and Processing

Adherent carbon film deposition by cathodic arc with implantation

E. G. Gerstner and D. R. McKenzie
School of Physics, The University of Sydney, Sydney NSW 2006, Australia

M. K. Puchert and P. Y. Timbrell
Surface Science and Technology, School of Chemistry, University of New South Wales, Kensington NSW 2033, Australia

J. Zou
Electron Microscope Unit, The University of Sydney, Sydney NSW 2006, Australia

(Received 19 April; accepted 5 November 1994)

A method of improving the adhesion of carbon thin films deposited using a cathodic vacuum arc by the use of implantation at energies up to 20 keV is described. A detailed analysis of carbon films deposited onto silicon in this way is carried out using complementary techniques of transmission electron microscopy and x-ray photoelectron spectroscopy (XPS) is presented. This analysis shows that an amorphous mixing layer consisting of carbon and silicon is formed between the grown pure carbon film and the crystalline silicon substrate. In the mixing layer, it is shown that some chemical bonding occurs between carbon and silicon. Damage to the underlying crystalline silicon substrate is observed and believed to be caused by interstitial implanted carbon atoms which XPS shows are not bonded to the silicon. The effectiveness of this technique is confirmed by scratch testing and by analysis with scanning electron microscopy which shows failure of the silicon substrate occurs before delamination of the carbon film. © *1995 American Vacuum Society.*

I. INTRODUCTION

The usefulness of thin films in many applications depends on the degree of bonding between the film and the substrate. This bonding may be improved by energetic bombardment, where some of the depositing atoms are driven into the substrate in order to provide an interface of graded composition between film and substrate. To do this successfully it is necessary to bombard with ions of sufficient energy to give the desired implantation, as well as provide a higher flux of lower energy ions for an adequate deposition rate. One must also ensure that both the energetic and nonenergetic ions are of the same type to avoid contamination of the film with foreign species.

We report here on a process which achieves this aim by using a filtered cathodic arc as a source of relatively low energy ions ($<$100 eV), and a pulsed high voltage substrate bias (up to -20 keV) to enable implantation of a fraction of these ions. Specifically, we use transmission and scanning electron microscopy and x-ray photoelectron (XPS) depth profiling to examine the microstructure and interfacial regions of highly adherent carbon layers deposited onto (100) silicon substrates by this technique.

Carbon was chosen for study because of widespread interest in it as a wear resistant and protective coating. Silicon was chosen as the substrate due to its availability as a large area single crystal of high purity, making it useful for the study of implantation phenomena.

II. EXPERIMENT

Cathodic or vacuum arcs provide a convenient source of plasma from a solid source.[1] The plasma is highly ionized but contains some neutral species and fragments of cathode material (macro-particles) that cause imperfections if incorporated into deposited films. A curved magnetic solenoidal filter has been devised by Aksenov and co-workers[2] which effectively removes both neutral atoms and macro-particles. The apparatus used here is shown in Fig. 1, and combines a filtered cathodic arc deposition source with a high voltage power supply and capacitor bank rated at 20 kV and 100 mF. The voltage is applied to the substrate which is held by means of a retaining ring with rounded corners. The shaft is surrounded by a clear glass tube to limit unwanted discharge onto the stem of the substrate holder.

Silicon (100) oriented substrates were clamped to the copper substrate holder, providing thermal anchorage as well as electrical contact. The substrate temperature during deposition lay in the range 300–320 K. The films were deposited by raising the substrate holder to -20 kV in vacuum, then triggering and operating the cathodic arc for 10 s. The applied bias voltage decreases exponentially with a time constant of 100 ms after triggering so that approximately 0.7% of the incident carbon ions has a kinetic energy ranging between 10 and 20 keV. After each 10 s deposition, the arc was turned off and the supply capacitors allowed to recharge (which took about 15 s). This process was repeated until the desired thickness was achieved. The time averaged deposition rate was approximately 30 nm/min. A film thickness of 30 nm was chosen for detailed study.

$\langle 110 \rangle$ cross-sectional transmission electron microscopy (TEM) specimens were prepared by face to face gluing with epoxy resin, mechanical thinning, and ion beam thinning. Specimen microstructures were investigated by a Philips EM430 transmission electron microscope operating at 300 kV.

X-ray photoelectron spectra were collected using a Kratos Axis/800 hemispherical energy analyzer equipped with an unmonochromatized Mg Kα x-ray source ($h\nu$=1253.6 eV). The binding energy scale was calibrated against Ag 3d5/2 at 368.25 eV and the instrumental energy resolution, measured

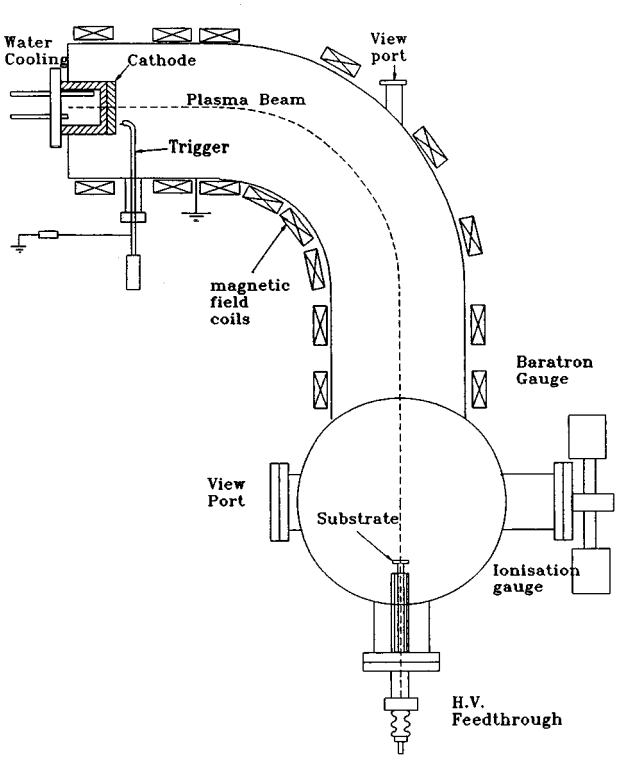

FIG. 1. The apparatus combining cathodic arc deposition with high voltage implantation used to deposit the adherent carbon films on silicon substrates.

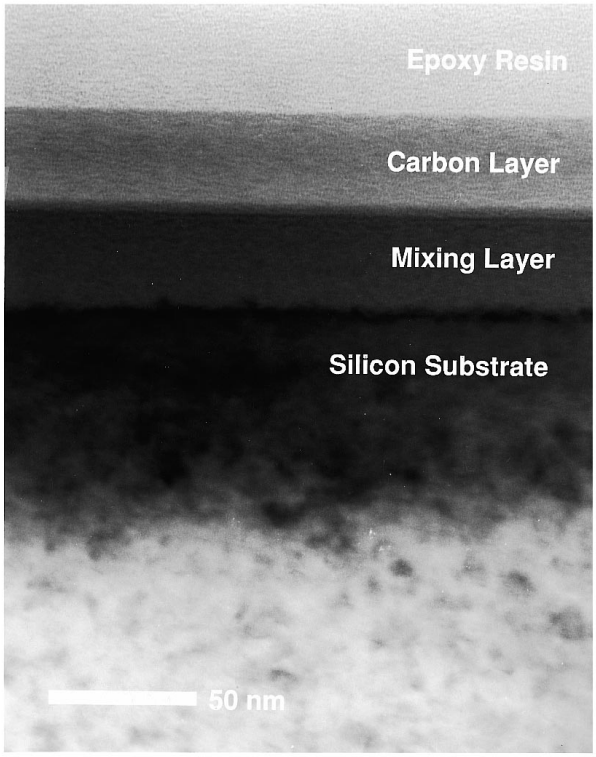

FIG. 2. A bright field TEM image showing the epoxy resin used in the specimen preparation, the amorphous carbon layer, the amorphous mixing layer, and the silicon substrate.

using the same peak, was 0.9 eV (pass energy set at 20 eV). Sample charging was minimized by bonding the substrate to a sample mount with a silver epoxy. Sputter depth profiling of the sample was performed with an Ar ion gun (5 keV, 12–14 μA sample current) in the XPS analysis chamber. The XPS analysis area was approximately 4×6 mm^2 on the sample, while the depth profiling crater was measured as 8×10 mm^2. Argon ion etching was halted periodically while XPS wide scans and detailed O 1*s*, C 1*s*, and Si 2*p* line shape spectra were recorded in order to provide both an elemental depth profile as well as a *chemical* (Si–C, C–C, Si–Si bond percentages) depth profile.

III. RESULTS

A. TEM investigations

Figure 2 is a bright-field image showing three distinct layers. The bottom region consists of crystalline silicon, as deduced from its electron diffraction pattern, while the upper two layers are amorphous. Epoxy resin is visible as an additional amorphous region above these two amorphous layers. The lower of these two amorphous layers we shall refer to as the ''amorphous mixing layer'' as it contains both silicon and carbon atoms (evidence of which will be shown later), and the upper one is essentially a pure amorphous carbon film as will be shown by the XPS results.

Figure 3 is a high resolution electron microscopy (HREM) image showing the interface region between the crystalline silicon and the amorphous mixing layer. Near the interface, there is a directionality in the image of the amor-

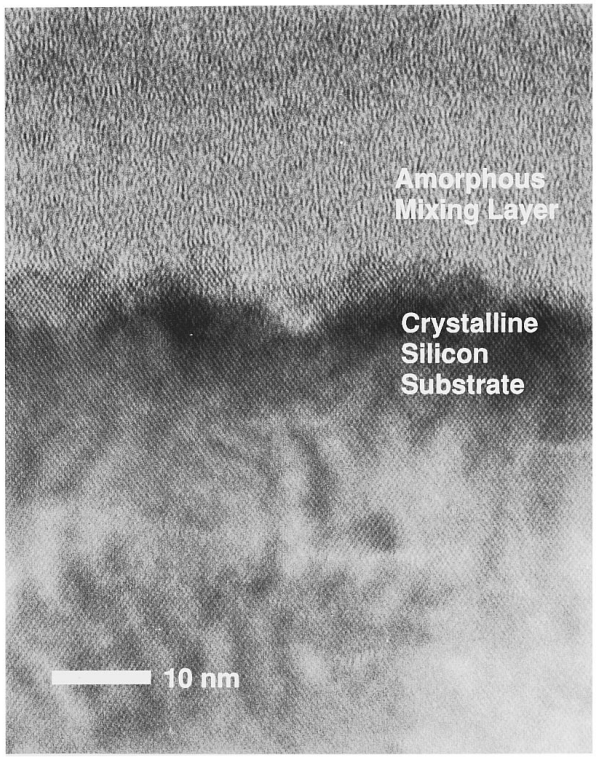

FIG. 3. A ⟨110⟩ HREM image showing the interface region between the crystalline silicon substrate and the amorphous mixing layer.

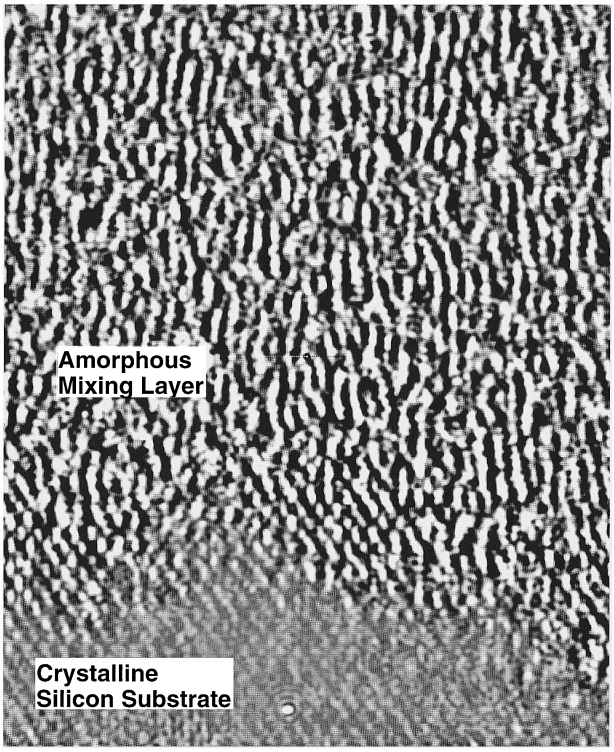

FIG. 4. A processed image of Fig. 3 which shows the ''directionality'' in the amorphous mixing layer, believed to be the result of upward flow during implantation.

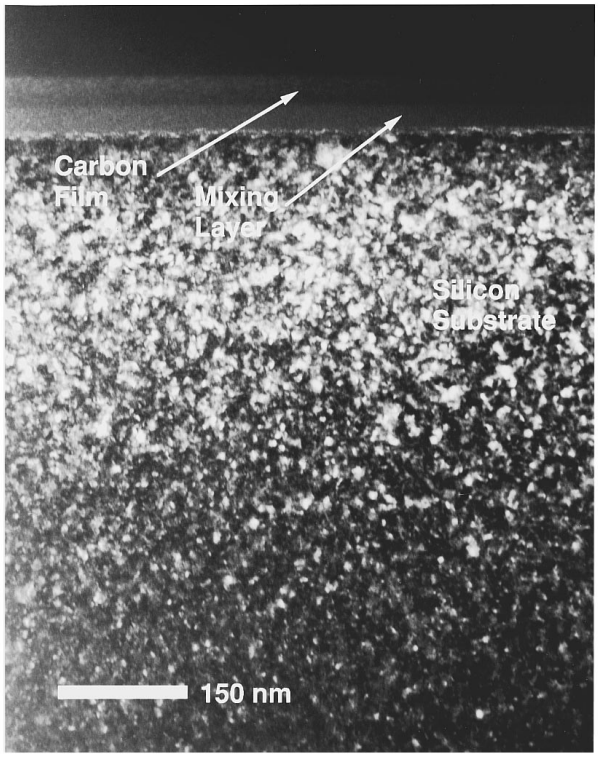

FIG. 5. A 220 weak-beam image (g/3.2g condition) showing that, in the silicon substrate, near the interface (to a 40 nm depth), few defects are found; in the region of 50–400 nm, an extended peak damages region is observed.

phous mixing layer that is not due to objective lens astigmatism. This directionality is emphasized by carrying out an image processing step in which the Fourier transform is calculated, the central spot of the transform masked out to increase contrast, and the result back-transformed to another image. This processed image is shown magnified in Fig. 4, showing clear vertical fringes in the mixing layer. These vertical fringes are interpreted as the result of vertical ''flow'' of the material as it expands during the insertion of large quantities of carbon into the silicon. This material must flow vertically as it is constrained in the horizontal direction.

Figure 5 is a 220 weak-beam image (under the image condition of g/3.2g). It is seen that the region extending down to a depth of 40 nm from the interface between the amorphous mixing layer and the substrate is actually darker, suggesting that not many defects exist in this region. However, many defects are found in the region of 50–400 nm, indicating that this region corresponds to the peak damage region. Two questions arise: (1) Why is there an extended peak damage region and (2) why is there a region within the top 40 nm that shows less damage? In connection with the first question, we note that the energy of ion bombardment varies from relatively low (<100 eV) to 20 keV during the discharge of the capacitor bank. Since the position of the peak damage depends upon the ion bombardment energy, it is not difficult to understand the reason for the extended peak damage region. However, the calculated range of the 20 keV C ion into the Si substrate of 47 nm appears lower than we observe.[3] In connection with the second question, for lower ion bombardment energies, it appears that the C ion may implant into the Si substrate to a high dose (see Sec. III B) without causing substantial damage to the substrate. Further work is needed to understand this phenomenon.

B. XPS Depth Profiling

The results of the XPS sputter depth profile are shown in Fig. 6. Atomic concentration profiles for silicon, carbon, and

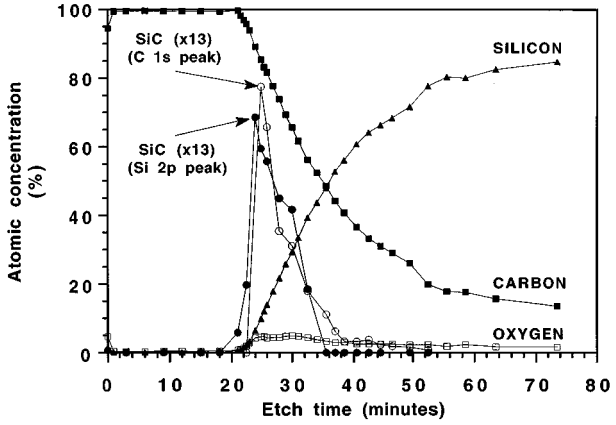

FIG. 6. The XPS sputter profile of the complete carbon/silicon system. The purely amorphous carbon film region ends at ~21 min total etch time. The regime of Si–C bonding is shown to be a relatively narrow region in the amorphous mixing layer (Si–C bond percentages scaled up 13×, measured using deconvoluted components in the Si 2*p* and C 1*s* peaks).

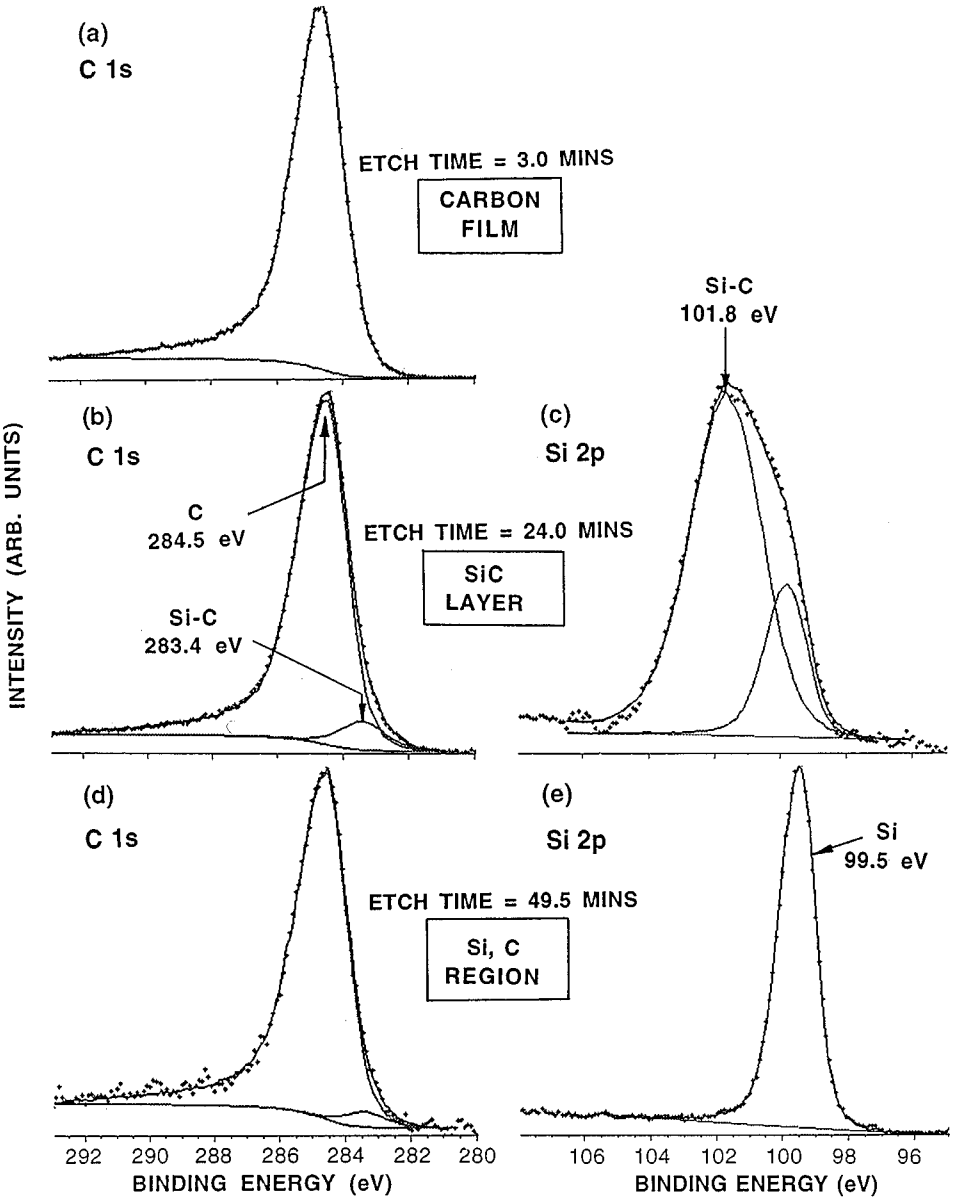

FIG. 7. C 1*s* and Si 2*p* spectra at the indicated etch times, corresponding to (a) the carbon film; (b), (c) the Si–C bonding region within the mixing layer; and (d),(e) the carbon implanted region in the silicon substrate.

oxygen are calculated from the total peak areas of the Si 2*p*, C 1*s*, and O 1*s* XPS peaks and represent the total atomic concentration of each element irrespective of chemical bonding. The interface positions are inferred by assuming an approximately constant etch rate (1–2 nm/min) for the top two amorphous layers. The amorphous carbon layer contained no detectable silicon in its interior, but a trace amount of silicon (~1%) was measured on the sample surface. This could possibly result from ''internal sputtering'' from the silicon during film deposition and leading to some silicon atoms traveling back through the carbon layer and accumulating on the surface. A low level of oxygen (~0.4%) was present throughout the carbon layer, probably due to background oxygen in the deposition chamber.

Higher resolution XPS scans (20 eV pass energy) of the Si 2*p* and C 1*s* line shapes reveal the atomic percentages of Si–C, C–C, and Si–Si bonds as a function of film depth. Representative Si 2*p* and C 1*s* spectra are shown in Fig. 7 for three regimes of the depth profile. Figure 7(a) is the C 1*s* peak for pure elemental carbon within the top amorphous layer after an etch time of 3.0 min. The tail on the higher binding energy side of this peak is mainly attributed to the intrinsic line shape of glassy carbon,[4,5] but may also reflect carbon bonding with the small amount of oxygen in the film (C—O and C═O functional groups). This intrinsic line shape was used in the deconvolution of later C 1*s* features where SiC components appear. Similarly, the intrinsically asymmetric Si 2*p* peak from a pure silicon (100) reference sample was used as the silicon XPS line shape model.

The silicon substrate was first detected after a total sputter time of 21 min (Fig. 6). From this point until 24 min total etch time, the Si 2*p* line shape [see Fig. 7(c)] was dominated

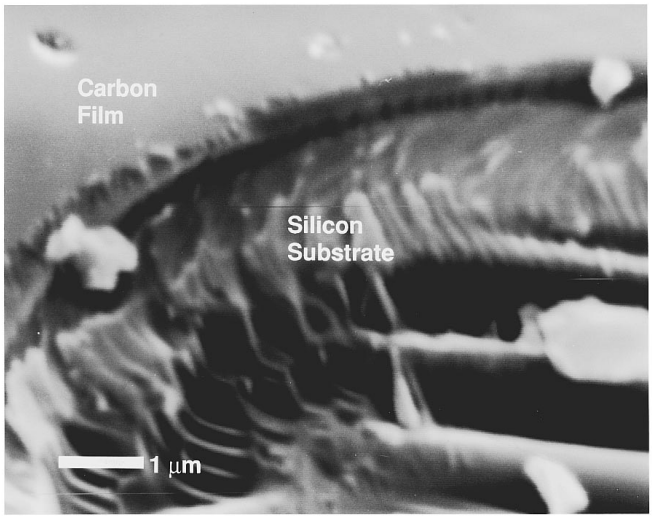

FIG. 8. A scanning electron micrograph showing the failure mode during scratch testing. No adhesive failure or delamination is revealed between the carbon layer and the darker amorphous mixing layer or between the amorphous mixing layer and the substrate.

by a component at 101.8±0.2 eV, consistent with the peak position[6] for SiC, with a lesser component at 99.5±0.2 eV and corresponding to elemental silicon. The presence of SiC at this stage is also confirmed by a C 1*s* component [Fig. 7(b)] at 283.4±0.2 eV, in good agreement with reported values for SiC.[7] The two plots of SiC bond percentage, shown scaled up in Fig. 6, are derived from the areas of the SiC components in the Si 2*p* and C 1*s* peaks, and there is a good agreement between these plots. This data indicate that direct Si–C bonding occurs within the amorphous mixing layer. With further depth profiling [Figs. 7(d) and 7(e)], carbon and silicon only appear in elemental forms.

C. Scratch testing

The result of scratching the film surface with a scratch testing machine is shown in the scanning electron micrograph of Fig. 8 for a carbon film of 150 nm thickness. The carbon surface layer and the darker amorphous mixing layer are visible as distinct layers with different contrast levels in this secondary electron image. Examination of many such craters showed that the failure in all cases was due to cracking of the silicon substrate underneath the amorphous layers, indicating strong bonding of the carbon layer to the substrate. This adhesion was for superior to that shown by carbon films deposited without implantation. Carbon films deposited by cathodic arc or by electron evaporation of graphite, without implantation, showed spontaneous detachment for a thickness of 100 nm or greater.

IV. A STRUCTURAL MODEL FOR THE LAYERS

The XPS profile data and the TEM investigations enable an interpretation of the carbon film structure and formation mechanism to be made. The damaged silicon substrate contains carbon that is not bonded to the silicon. The carbon atoms are clearly excluded from the majority of the crystalline silicon, which shows normal silicon diffraction patterns. The carbon must therefore lie around the edges of the silicon blocks in segregated carbon zones.

The cross-sectional view of the structure shows the effects of an increasing carbon dose in the silicon substrate as the observation point is moved upward. At a certain level, the carbon dose will be sufficient to amorphize the silicon, a well-known phenomenon in ion damage studies.[8] This transition is the reason for the crystalline-to-amorphous interface which defines the lower surface of the amorphous mixing layer. The XPS profile shows that mixing extends well into the crystalline silicon substrate. In fact, the damage produced by such mixing may lead to weakness in the silicon, and the evidence from scratch testing shows that the silicon substrate is, in fact, the weakest part of the coated structure.

The carbon content continues to increase monotonically upward through the amorphous mixing layer. The presence of a minority phase (not exceeding 6 at. %) of SiC occurs within this layer. Freed from the constraint of a crystalline silicon matrix, bonding can readily occur between silicon and carbon atoms in the amorphous state. The expansion necessary when carbon enters the silicon in substantial quantities is probably responsible for the pronounced anisotropic texture in this layer, as was discussed previously.

The lower interface between the amorphous mixing layer and the crystalline interior region is rough. This is the result of point-to-point variations in the carbon ion dose and leading to the amorphous-to-crystalline transition at different depths. The upper interface of the amorphous mixing layer with the carbon film is quite smooth. This interface, we believe, represents the original silicon surface, displaced upwards from its initial position by the insertion of carbon into the silicon lattice. The silicon concentration falls to zero above this line, and the directionality in the image disappears. These observations are entirely consistent with an upward ''flow'' of the mixing layer.

V. CONCLUSIONS

We have demonstrated the feasibility of a cathodic arc deposition process combined with high voltage implantation as a means of promoting the formation of a mixing layer containing atoms of the substrate and the depositing material. Scratch testing of a carbon film deposited onto a silicon substrate reveals that the degree bonding of the deposited film to the mixing layer and of the mixing layer to the substrate is very high. However, failure occurs in the substrate probably because of implantation damage. The possibility of improving the performance of the carbon/silicon combination by annealing out the damage in the silicon needs to be investigated. Similar improvements in film adhesion using this technique should be obtainable with other film/substrate ma-

terials. Improvements will, however, rely on the nature of the mixing layer and the damage to the substrate dependent on the solubility of the respective materials with one another.

ACKNOWLEDGMENTS

The authors wish to thank Ela Kravtchinskaia for depositing the carbon films, Adam Sikorski for preparing the cross-sectional TEM specimens, and C. R. Howlett and J. C. Kelly for valuable discussions and assistance.

[1]W. D. Davis and H. C. Miller, J. Appl. Phys. **40**, 2212 (1969).
[2]I. I. Aksenov, V. A. Belous, V. G. Padalka, and V. M. Khoroshikh, Sov. J. Plasma Phys. **4**, 425 (1978).
[3]B. Smith, *Ion Implantation Range Data for Silicon and Germanium Device Technologies* [Learned Information (Europe), Oxford, 1977].
[4]T. T. P. Cheung, J. Appl. Phys. **53**, 6857 (1982).
[5]T. T. P. Cheung, J. Appl. Phys. **55**, 1388 (1984).
[6]I. Kusunoki and Y. Igari, Appl. Surf. Sci. **59**, 95 (1992).
[7]D. R. Wheeler and S. V. Pepper, Surf. Interface Anal. **10**, 153 (1987).
[8]R. J. Schreulelkamp, J. S. Custer, J. R. Liefting, W. X. Lu, and F. W. Saris, Mater. Sci. Rep. **6**, 275 (1991).